Fig. S1

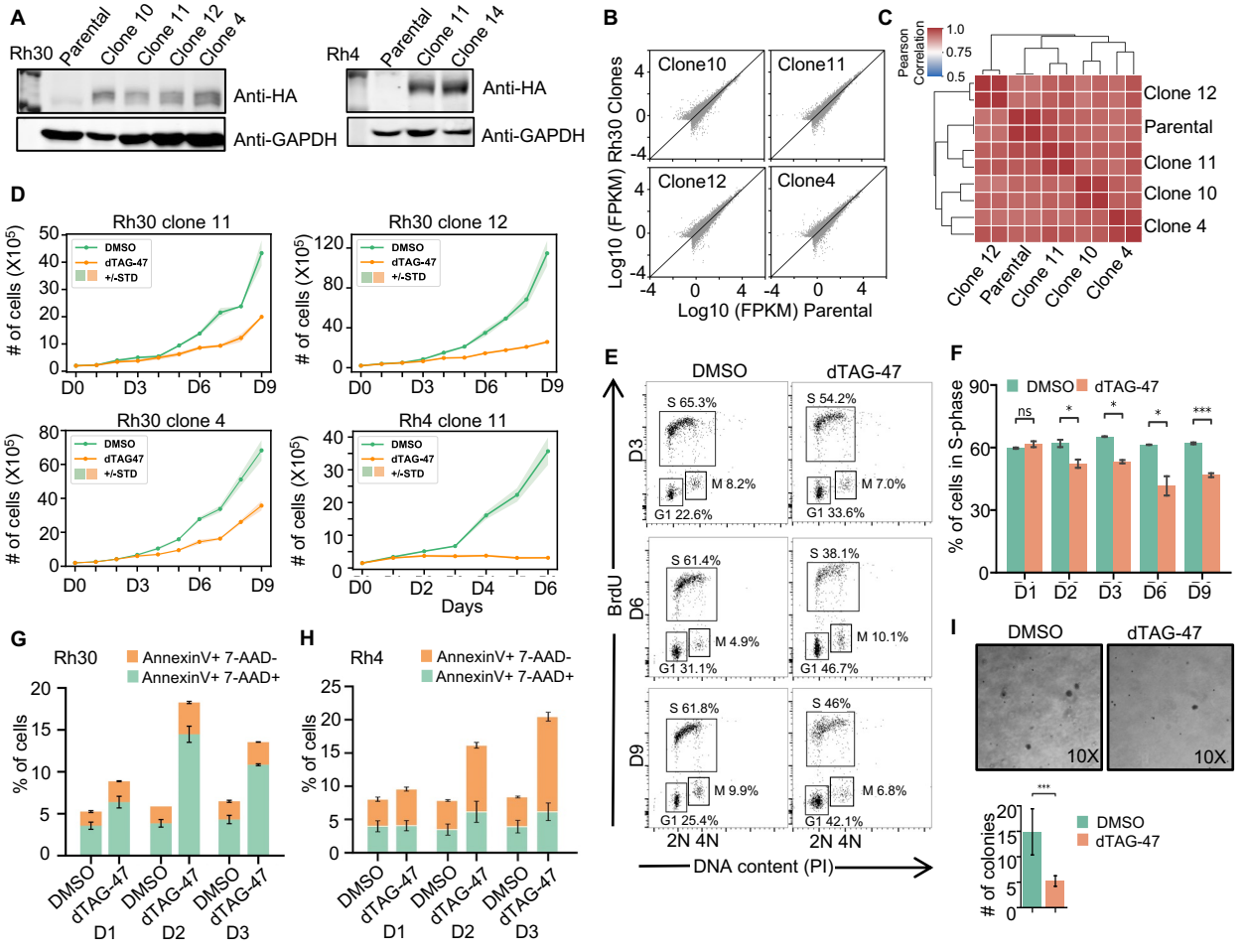

Figure S1. Degradation of PAX3-FOXO1-FKBP triggers cell death and differentiation, Related to Figure 1. (A) Western blot analysis of four Rh30 PAX3-FOXO1-FKBP clones and two Rh4 PAX3-FOXO1-FKBP clones. (B) Scatter plot of $\log_2$ normalized counts from RNA-seq across four different Rh30 PAX3-FOXO-FKBP clonal cell lines compared to parental Rh30 cells showing all expressed genes; n=2. (C) Cluster heatmap of Pearson correlations from RNA-seq of four different PAX3-FOXO-FKBP cell lines expanded from single cell clones and parental Rh30 cells. Each cell line has two biological replicates and data was normalized to total counts. (D) Growth curves of Rh30 PAX3-FOXO1-FKBP clones. Cells were treated with 500 nM dTAG-47, and cell counts were determined using Trypan Blue dye exclusion. Shading shows the mean ± STD (n=3). (E) Cell cycle analysis of Rh30 PAX3-FOXO1-FKBP cells. The cells were treated with 500 nM dTAG-47 for the indicated times before flow cytometry analysis for BrdU incorporation. Plots of BrdU versus propidium iodide (PI) shows fewer cells in S-phase and accumulation of cells in G_1-phase after dTAG-47 treatment. (F) Bar graph showing statistical analysis of biological replicates of cells in S phase from panel E. Data are presented as mean ± STD (n=3). (G and H) Apoptosis analysis of Rh30 (G) and Rh4 PAX3-FOXO1 cells (H). The cells were treated with 500 nM dTAG-47 for the indicated times before flow cytometry analysis for AnnexinV and 7-AAD staining. Data are presented as mean ± SEM (n=3). (I) Growth in soft agar. Rh30 PAX3-FOXO1-FKBP cells were pre-treated with 500 nM dTAG-47 for 6 days before plated in soft agar. 4 weeks later the number of colonies were counted using microscopy (4X). Representative images show colonies using an inverted microscope (10X). The bar graph displays colony counts with the bar the mean ± STD (n=9). (*p*, independent T test. *: *p* <= 5.0e-02, **: *p* <= 1.e-02, ***: *p* <= 1.0e-03, ****: p <= 1.0e-04).

Fig. S2

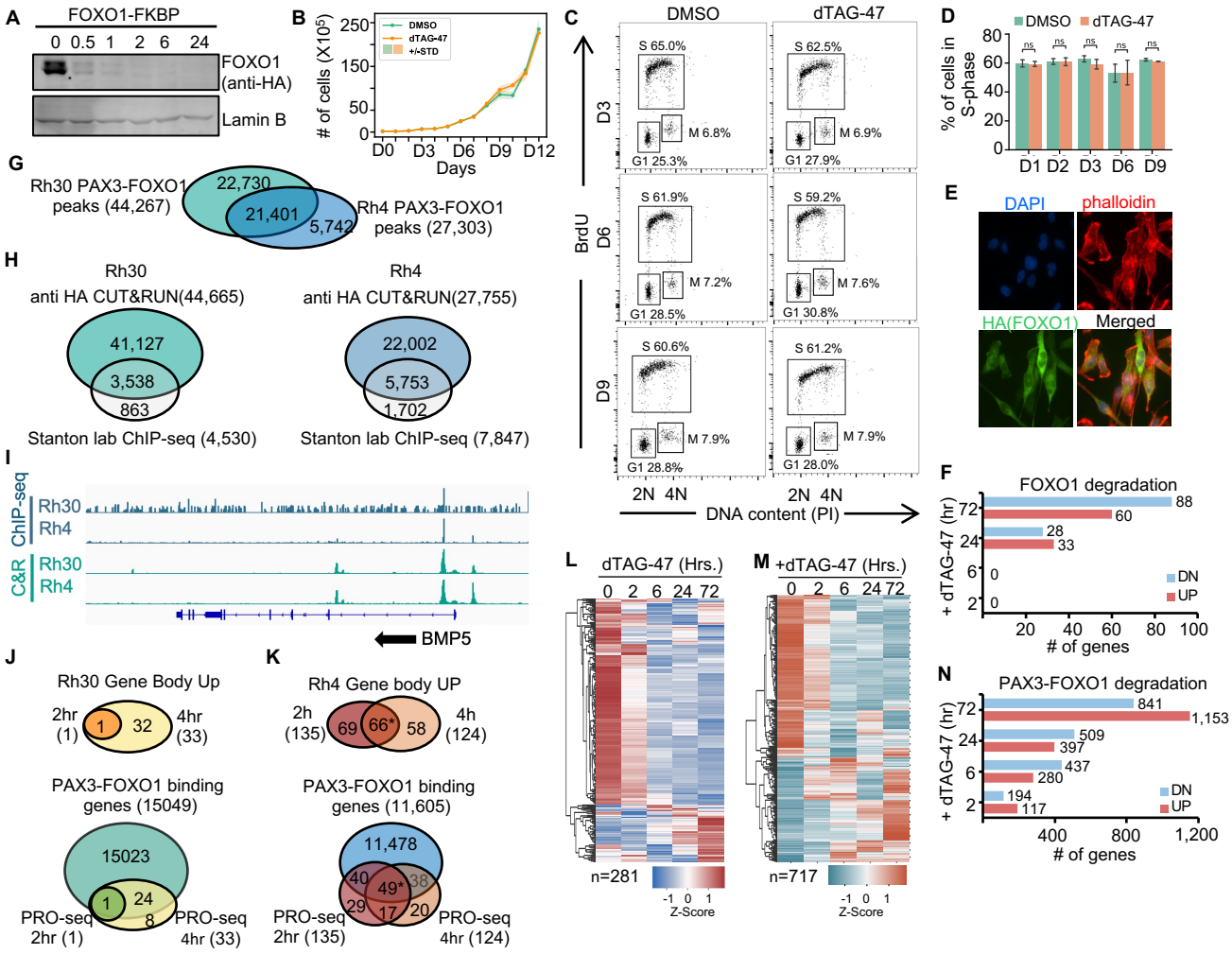

Figure S2. Analysis of PAX3-FOXO1-FKBP and FOXO1-FKBP cells, Related to Figure 1 and 2. (A) Western blot analysis of FOXO1-FKBP before and after degrading endogenous FOXO1-FKBP (upper panel). Lamin B was used as a loading control (bottom panel). (B) Cell proliferation of Rh30 FOXO1-FKBP cells was performed by treating with 500 nM dTAG-47, and cell counts were determined using Trypan Blue dye exclusion. Data are graphed as mean ± STD (n=3). (C) Flow cytometry analysis of incorporated BrdU versus PI in Rh30 FOXO1-FKBP cells after treatment of 500 nM dTAG-47 at Day-3, Day-6 and Day-9. (D) Bar graph showing the results of biological triplicate flow cytometry analysis showing no change in the percentage of cells in S-phase. Data are presented as mean ± STD (n=3; *p* derived from an independent T test. *: *p* <= 5.0e-02, **: *p* <= 1.0e-02, ***: *p* <= 1.0e-03, ****: *p* <= 1.0e-04). (E) Immunofluorescence staining of FOXO1 using anti-HA in Rh30 FOXO1-FKBP cells. DAPI was used to label nuclei (blue). Alexa 568-labeled Phalloidin was used to mark actin filaments (red). Alexa 488 secondary antibody was used to visualize the primary antibody against HA (green; magnification 100X). (F) Quantification of the number of genes changed at the indicated time points following FOXO1 degradation. (G) Venn diagram showing the overlap of PAX3-FOXO binding peaks between Rh30 and Rh4 (*: *p* <= 1.0e-10). (H) Venn diagrams showing the overlap of PAX3-FOXO1 binding site between the CUT&RUN and published ChIP-seq in Rh30 (left) and Rh4 (right) cells. (I) IGV gene tracks showing the PAX3-FOXO1 CUT&RUN and ChIP-seq at the *BMP5* locus. (J and K) Venn diagrams showing the PRO-seq signal quantified within the gene body with changes over time upon degradation of PAX3-FOXO1, and the overlap between PAX3-FOXO1 CUT&RUN and PRO-seq signal quantified within the gene body in Rh30 (J), or Rh4 (K) (*: *p* <= 0.05). (L and M) Heatmaps of RNA-seq plotted by the genes with PRO-seq gene body change (L), and mRNA changed after 6hr of dTAG-47 treatment (M) at indicated time points. (N) Bar graph showing the number of gene changes detected by RNA-seq after degrading PAX3-FOXO1 at indicated time points.

Fig. S3

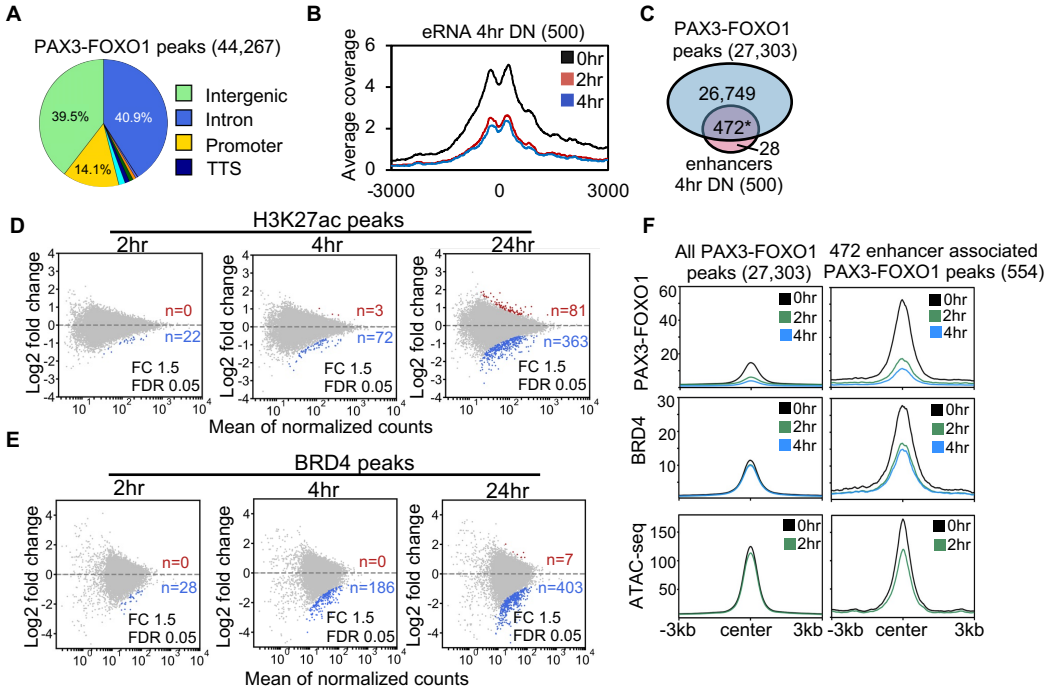

Figure S3. Gene expression and genomic analysis of PAX3-FOXO1-FKBP cells, Related to Figure 3. (A) Pie chart showing the annotation of PAX3-FOXO1 binding sites to gene features in Rh30 cells. (B) Histogram of PRO-seq reads around enhancer center after PAX3-FOXO1 degradation in Rh4 cells. (C) Venn diagram showing the overlap between PAX3-FOXO1 peaks and the down-regulated eRNA peaks at 4hr in Rh4 cells (*: p <= 1.0e-10). (D and E) MA-plots of H3K27ac (D) and BRD4 (E) peak changes from 2hr to 24hr after degrading PAX3-FOXO1 from Rh30 cells. (F) Histograms of the average signal of PAX3-FOXO1, BRD4, and ATAC-seq over a 4hr time course of dTAG-47 treatment over the regions encompassing all P3F bound sites versus those P3F sites associated with changes in eRNA transcription in Rh4 cells.

Fig. S4

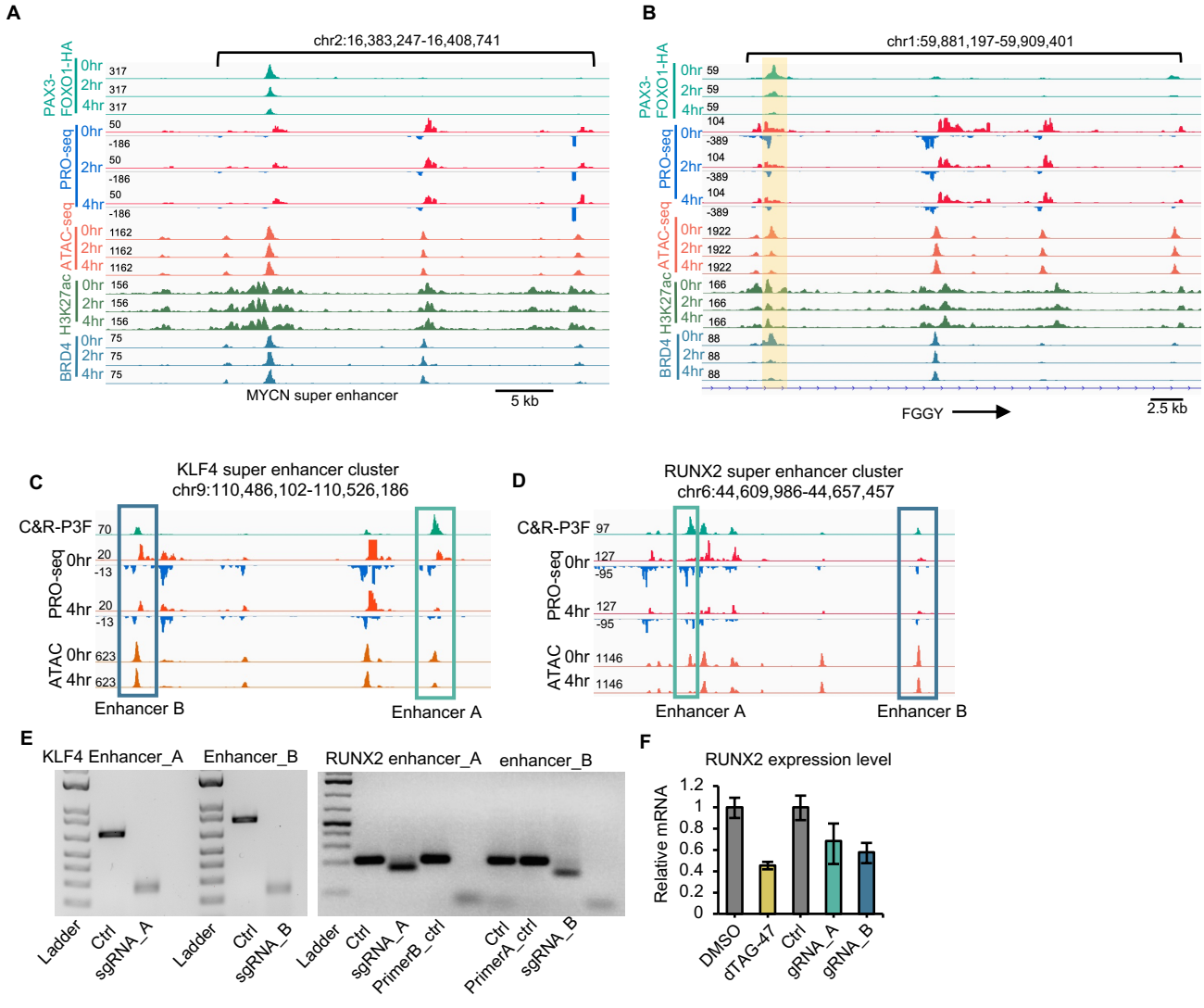

Figure S4. Intersection of CUT&RUN, PRO-seq and ATAC-seq analysis, Related to Figure 3. (A and B) IGV gene tracks showing the PAX3-FOXO1 CUT&RUN, PRO-seq, ATAC-seq, H3K27ac ChIP-seq, and BRD4 CUT&RUN at the super-enhancers associated with *MYCN* (A) and *FGGY* (B). (C and D) IGV gene tracks showing the PAX3-FOXO1 CUT&RUN, PRO-seq, ATAC-seq at the super-enhancers associated with *KLF4* (C) and *RUNX2* (D). Boxed regions showing the enhancers that were deleted in E and F. (E) Genomic PCR flanking the deleted enhancer regions indicated in C and D revealed a smaller PCR product generated by successful deletion. (F) Bar graph reveals the relative mRNA expression of RUNX2 gene with indicated treatment.

Fig. S5

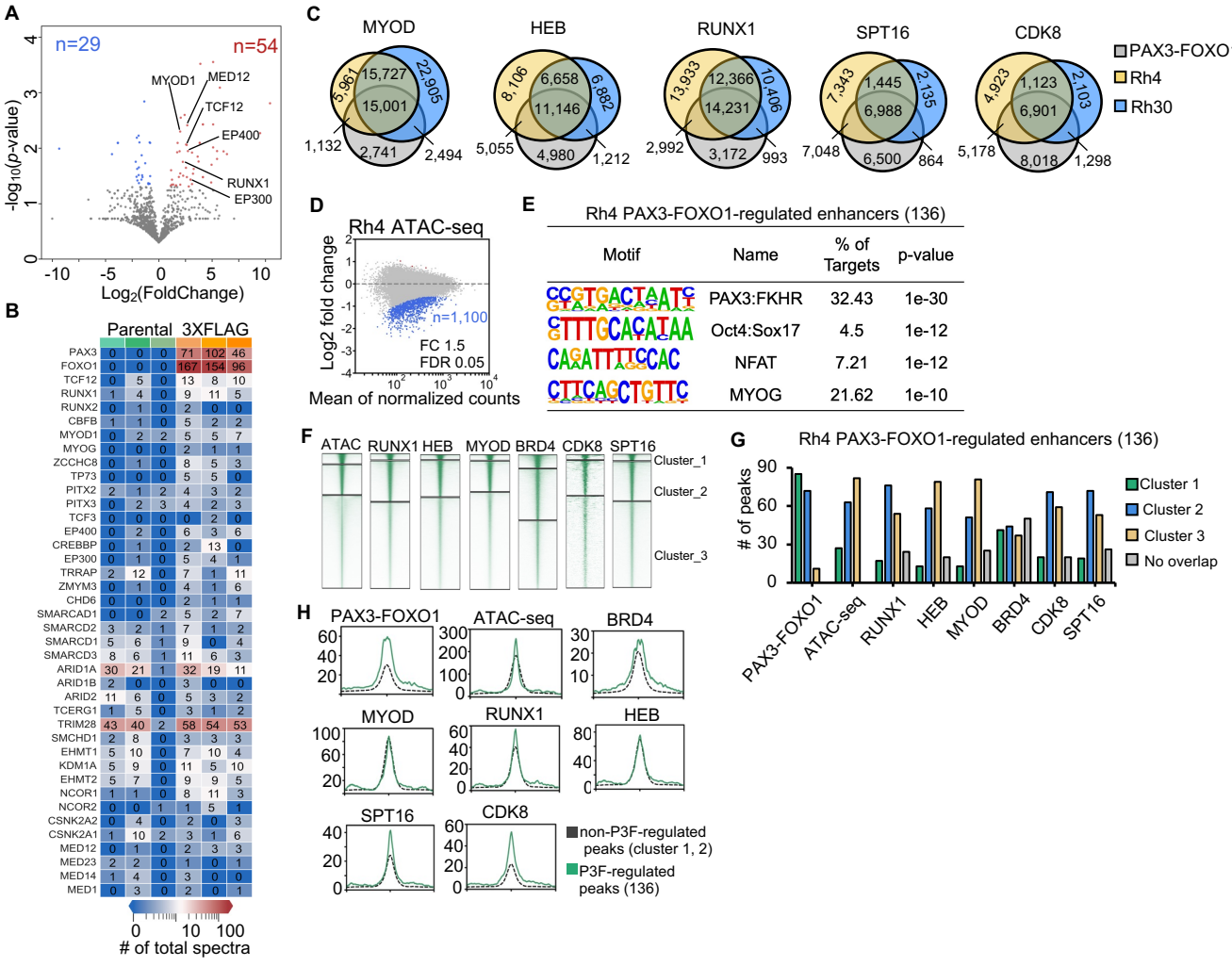

Figure S5. Proteomic analysis of PAX3-FOXO1-3XFLAG cells, Related to Figure 4 and 5. (A) Volcano plot generated from the mass spectrometry results of PAX3-FOXO1-3XFLAG immunoprecipitation/mass spectrometry. Proteins that purified with FLAG-M2 beads were plotted as log2 fold change (PAX3-FOXO1-3xFLAG/Parental) vs. -log10 of the p-value. The absolute 1.5-fold change and p-value 0.05 was used as the threshold (n=3 biological replicates, *p* calculated using one-tail unpaired T-test). Significant hits are depicted in blue and red to reflect proteins that are enriched in parental samples and PAX3-FOXO1-3XFLAG samples, respectively. (B) Heatmaps of selected PAX3-FOXO1-associated proteins from the 3XFLAG analysis. Spectral counts are shown within each box. (C) Venn diagrams display the overlap of MACS2 identified peaks from CUT&RUN analysis between PAX3-FOXO1 and the indicated factor in Rh30 and Rh4 cells. (D) MA-plot of ATAC-seq changes in Rh4 clone 14 cells treated with dTAG-47 for 2hr. (E) Motif analysis of the 136 ATAC-seq sites associated with genes down-regulated after PAX3-FOXO1 degradation. (F) Heatmaps showing the K-means clusters for each of the indicated factors from Rh4 cells. (G) Bar graph showing the number of high-confidence PAX3-FOXO1-regulated enhancer peaks (136) present in Rh4 data segmented based on K means clustered PAX3-FOXO1, ATAC-seq, RUNX1, HEB, MYOD, BRD4, CDK8, and SPT16 binding sites from Figure S5E. (H) Histograms of the CUT&RUN signal of the indicated factors around the regulated ATAC-seq peaks versus non-regulated peaks in Rh4 cells.

Fig. S6

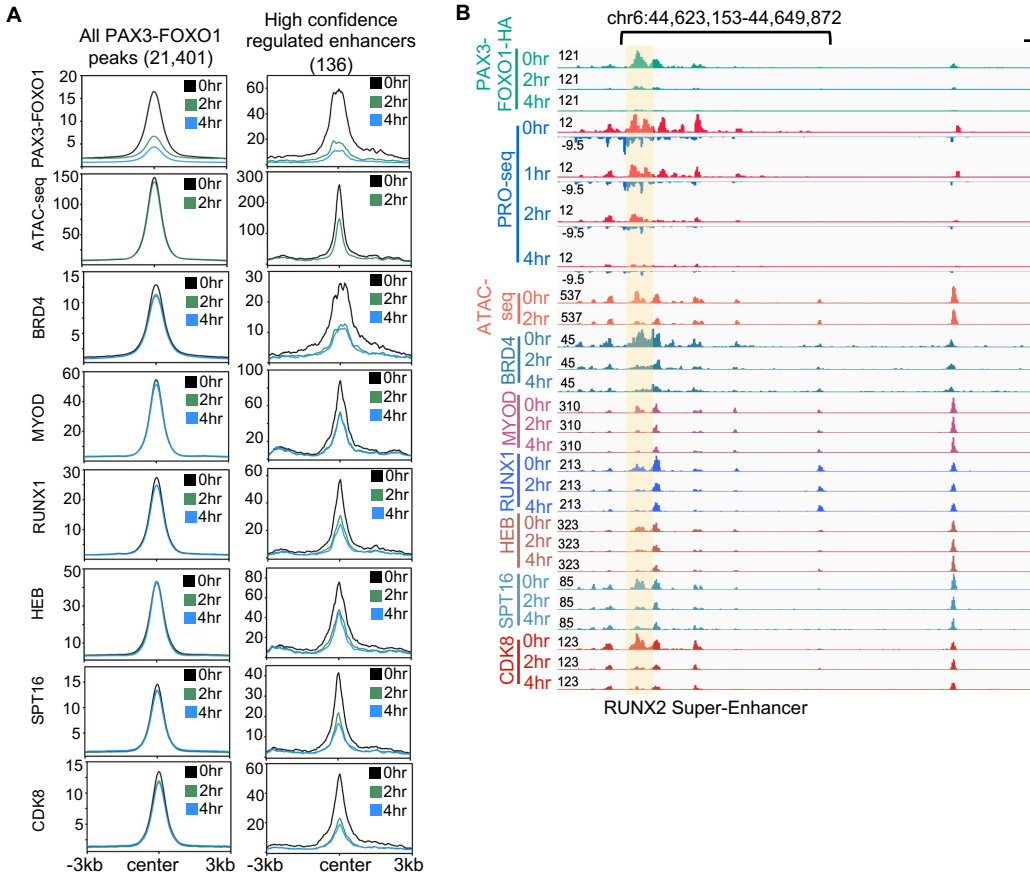

Figure S6. PAX3-FOXO1 is required for maintaining open chromatin at regulated enhancers in Rh4 cells, Related to Figure 6. (A) Histograms of the CUT&RUN signal of the indicated factors around all PAX3-FOXO1 peaks, the regulated ATAC-seq peaks in Rh4 cells. (B) Genome browser view of the *RUNX2* "super" enhancer in Rh4 cells. The shaded box highlights an enhancer showing changes in factor binding, eRNAs, and accessibility over time compared to neighboring enhancers.